

Brief communication

“Determination of urban growth in catchment areas in Cyprus using multi-temporal remotely sensed data: risk assessment study”

D. G. Hadjimitsis

Cyprus University of Technology, Department of Civil Engineering and Geomatics, Remote Sensing Laboratory, Lemesos, Cyprus

Received: 14 April 2009 – Revised: 22 October 2010 – Accepted: 22 October 2010 – Published: 8 November 2010

Abstract. The aim of this study is to quantify the actual urbanization activity near the catchment area in the urban area of interest located in the vicinity of the Agriokalamin River area of Kissonerga Village in Paphos District. Remotely sensed data such as aerial photos, Landsat-5/7 TM/ETM+ and Quickbird image data have been used to track the urbanization activity from 1963 to 2008. In-situ GPS measurements have been used to locate in-situ the boundaries of the catchment area. The results clearly illustrate that tremendous urban development has taken place ranging from 0.9 to 33% from 1963 to 2008, respectively. A flood risk assessment and hydraulic analysis were also performed.

1 Introduction

Land use and cover change and its impacts on the existing environment must be investigated and monitored on a systematic basis (Masek et al., 2000). Ecosystem and floods are closely related and any changes in the ecosystem, such as urbanization across the catchment’s area, may trigger off a sequence of flood occurrence causes. The causes of floods are closely interrelated to topological, meteorological, climatic, biological and hydrological factors (Zhang et al., 2007). Nevertheless, as witnessed by floods worldwide, land use and cover changes associated with human activities may affect the hydrological processes and increase flood risks (Khan, 2005; Brath et al., 2006). Expansion of human settlements and accompanying activities, especially the rapid

urbanization occurring in the developing countries, play an important role in global land use and cover change (Masek et al., 2000) that cause changes to ecological processes both regionally and globally.

Hydrological models have been widely used to calculate the hydrological parameters of a flood in order to estimate flood hazard (Niehoff et al., 2001). Remote sensing technology together with Geographic Information Systems (GIS) have become key for flood monitoring in recent years, by assisting the monitoring of urban growth (Townsend and Walsh, 1998; Hadjimitsis, 2007). The remote sensing techniques can be used to monitor the current situation before, during or after disasters like floods (Khan, 2005). Such image-data can be used to provide baseline data against which future changes can be compared, while GIS techniques provide a suitable framework for integrating and analyzing the many types of data sources required for disaster monitoring such as flooding (Hadjimitsis, 2007).

The permanent mapping and in-field surveying of the urbanized regions is not considered as the ideal monitoring tool for urban planners and local authorities. Remotely sensed imagery, in some cases, may be the only reliable source for a sufficient monitoring, as shown by other researchers (e.g., Moeller, 2005). Satellite-acquired image data provide a synoptic overview for large regions, recorded always with a standardized and calibrated monitoring system. The availability of cloud free images for operational projects is very important and depends on the geographical position and the prevailing weather conditions for the area of interest. Countries such as Greece and Cyprus are characterized by good weather conditions and the availability of cloud-free images. This is important when using satellite remote sensing in multi-temporal studies of those areas. The number of available cloud-free images of Cyprus per year is



Correspondence to: D. G. Hadjimitsis
(d.hadjimitsis@cut.ac.cy)

very high. It is apparent that the availability of cloud-free images of Cyprus increases the potential of using satellite remote sensing techniques.

This paper examines the potential for using satellite remote sensing techniques in Cyprus (which is made attractive by the frequency of high cloud-free imagery availability and moreover due to the fact that a single Landsat TM/ETM+ image of Cyprus covers almost the entire island), and attempts to explore the need for monitoring urban expansion on a catchment scale by integrating remote sensing, hydrological and meteorological data and hydraulic analysis, with the aim to apply them in a flood risk assessment study.

2 Methodology and study area

2.1 The method

The overall methodology of this project is based on the use of remote sensing for monitoring urban growth as well on the use of hydraulic analysis for implementing a risk assessment study for flood events across catchment areas.

After defining the catchment area using topographic maps and a digital elevation model, a GIS software, such as ARCVIEW (<http://www.esri.com/>) is required to measure the catchment area. Subsequently, pre-processing of the available remotely sensed images is required. Emphasis is given in ortho-rectification and radiometric correction (including atmospheric correction) to the Landsat TM/ETM+ imagery. For the post-processing of satellite imagery, an overlay algorithm is used based on the area of interest and the following different available land-cover change algorithms are implemented: the Maximum Likelihood Supervised Classification technique for the recent acquisitions and unsupervised classification for old acquisitions. The urbanization factor (in %) is then determined for each image acquisition. This factor denotes the amount of building activities occurred in the area under investigation and includes all the pixels in the scene that are not agricultural, water, grassland (i.e. buildings, asphalt areas, concrete areas, sand, etc.).

The final step of the proposed methodology is the application of a hydraulic analysis in order to retrieve the return period of a flood event and then perform a risk assessment study. Hydraulic analysis was used to model the flood prone areas and to compute the depth and duration of flooding in different sections. Hydrological analysis requires hydrological and meteorological data for the assessment of flood hazards, such as water level and discharge hydrographs, rainfall amounts, evaporation, temperature etc. Based on hydraulic analysis and all related information, maps have been established that for different scenarios display, the flood extent and the water depths/water levels (mapping performed through GIS technology).

2.2 The study area

The study area is the catchment scale in Agriokalamini River located in the vicinity of the following villages of the southwest part of the Paphos District area in Kissonerga, Tala, Emba, Kili and Tremithoussa Villages (located southwest of Paphos) as shown in Fig. 1.

3 Remote sensing data: pre-processing and post-processing

3.1 Remote sensing data

An ortho-rectified aerial photograph acquired on 1963, five Landsat TM/ETM+ images acquired on 1985, 1987, 2000, 2001, 2008 and two high-resolution Quickbird images acquired on 2003 and 2006 were used in this study. The ERDAS Imagine 2010 software (<http://www.erdas.com>) has been used for the processing of the available satellite images.

3.2 Pre-processing

The following pre-processing steps have been applied to the series of satellite images:

Geometric correction: geometric correction was carried out using standard techniques with ground control points and a first order polynomial fit (Mather, 2004). Twenty well-defined features in the images such as road intersections, corners of large buildings were chosen as ground control points. Topographical maps of 1:5000 scale have been used to track the position of each ground control point (GCP). To get precise ortho-correction image, we collected coordinate values of GCP corresponding to specific points of satellite image using files of 1/5000 Topographic Map and DEM files (10 m intervals).

Radiometric correction: satellite images were converted from digital numbers to units of radiance using standard calibration values. Then the at-satellite radiance values were converted to at-satellite reflectance values using the solar irradiance at the top of the atmosphere, Sun-Earth distance correction and solar zenith angle (Mather, 2004). In this study, the darkest pixel atmospheric correction method was applied to every image (Hadjimitsis et al., 2004a, b). It has been found that atmospheric effects contribute significantly to the classification technique. So the darkest pixel atmospheric correction method has been applied to the available images.

3.3 Post-processing: unsupervised and supervised classification

Classification has mainly been applied to the series of satellite images as a post-processing process. The following five classes have been used as “training classes” for both the “supervised and unsupervised classification algorithms”:

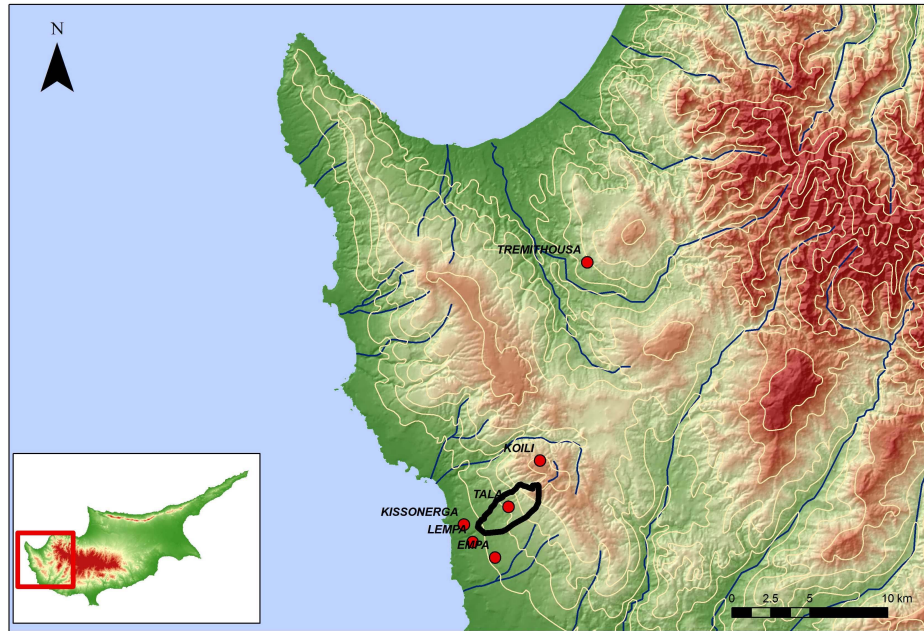


Fig. 1. A geomorphological view of the study area consisting of five nearby villages located in the Paphos District Area in Cyprus.

(1) vegetation, (2) asphalt area, (3) urban area which denotes any land cover with whitish or grey colour or urban area that denotes buildings (white high reflectance values), (4) water surfaces, and (5) bare soil.

Unsupervised classification is a statistical clustering analysis with its main task being to separate image pixels into groups of similar spectral characteristics (Mather, 2004). A pixel is classified on the basis of its value. The process includes the following: (a) designation of the total class numbers N to be grouped; in this study, five classes are used; (b) N seeds are generated to initialize the grouping process; (c) the pixel with a value similar to the seed will be grouped into the class of the seed; (d) the class mean is computed for all the pixels belonging to the same class; (e) an iteration between the previous two steps is applied automatically until no significant change taking place.

The selected classes can be compared to the ground truth in order to obtain the attribute of each class. Some of the classes can be merged together on the basis of the knowledge of ground truth. Some minor classes can be deleted. In this case, based on the fact that the selected classes have differences in their reflectance characteristics, this cannot occur but, as it is expected in the unsupervised classification, some mixing of the pixels into different classes could be occurred.

Supervised classification is a procedure for identifying spectrally similar areas on an image by identifying “training” sites of known targets and then extrapolating those spectral signatures to other areas of unknown targets. Training samples are taken to obtain statistics of known classes

(Mather, 2004; Hsiao et al., 2004). The most popular classifier is the Maximum Likelihood classification which has been applied in the present study area. The premise of this approach is the normality of the spectral distribution of pixel values for each land-cover type.

The five selected classes used are based on the distinctive spectral signatures. It is important to highlight that the reason that the author applied both of the classification techniques was that since archived satellite image data have been already used in this study such as images acquired on 1985 and 2000, the unsupervised classification technique was implemented due to the lack of accurate land-cover mapping. Supervised classification was also applied especially on the new acquisitions for example for the 2008 image acquisition since on-site visits have been performed and the existing classes have been retrieved on spot. Land-survey maps, topographical maps and town-planning records and data from the national Corine records have been used to support our classification results.

Spectro-radiometric measurements of similar classes acquired over the 2008 using GER1500 field spectro-radiometers (Hadjimitsis and Themistocleous, 2009) are used as a basis for assessing the results of the unsupervised classification, despite of the fact that such measurements have not been acquired during the satellite overpass. For example, the Remote Sensing Laboratory of the Cyprus University of Technology has already developed a database of the spectral signatures of several targets under the local conditions based on the large-scale spectro-radiometric campaigns. Targets such as asphalt, bare soil, eutrophic

inland waters are considered as non-variant targets with the following average reflectance values: (a) asphalt: 10% for TM band 1, 11.60% for TM band 2, 12.56% for TM band 3 and 14.56% for TM band 4; (b) bare soil: 11.63% for TM band 1, 15.04% for TM band 2, 16.18% for TM band 3 and 16.82% for TM band 4; (c) eutrophic inland water (lakes, rivers) 5% for TM band 1, 3% for TM band 2, 2.5% for TM band 3 and 3% for TM band 4. Vegetation target cannot be considered as non-variant target and the accuracy assessment was only performed using the above three targets (that correspond to the selected classes).

4 Analysis of data

4.1 Risk assessment

Flood risk is a function and a product of hazard and vulnerability (Ologunorisa, 2004). Flood risk is a result of the combination of the flood hazard and the consequences of the flooding. Indeed, a vulnerability analysis allows the identification of the population and infrastructures at greatest risk from flooding. Firstly, information about the flood hazard and the communities at risk has been gathered. Secondly the physical flood areas have been overlaid with the vulnerable areas. Flood hazard and vulnerability maps are used to produce flood risk maps. Severe flood risk zones and low flood risk zones have been identified using GIS software, like the ARCVIEW.

The European Flood Directive recommends the creation of flood risk maps with different hazard criteria, (1) flood events with a high probability (HQ 10), (2) flood events with a medium probability (HQ 100), and (3) flood events with a low probability (extreme event). This risk assessment study includes information on water depth and velocity as well as areas with embankment erosion and sediment deposit. Critical water depths and velocities had been explored and were derived from hydrodynamic models in order to derive hazard intensity. Such values were in an additional step used for the creation of risk maps. Vulnerability values varied between low (such as agricultural areas), medium (such as small villages), and high values (building development zones).

4.2 Meteorological data and hydraulic analysis

Rainfall values have been collected for all the sub-catchment areas as reported by the Pafos Meteorological Station for the incidence of 30 October 2006 between the hours 19:00 and 20:10 (LT). The intensity of rain was low at the beginning of storm between the hours 19:00 and 19:40. The total duration of storm was 70 min and was terminated in 20:10. An estimation of the maximum rainfall intensity at selected periods of 5 (e.g. 19:45 and 19:50), 10, 15, 30, 60 min intervals was made. Indeed, the maximum rainfall intensity

was recorded between 19:45 and 19:50 with total amount of recorded rain was of 11.5 mm, while between 19:40 and 19:50 the recorded amount of rain was 17.5 mm; 78% of rainfall (40.9 mm) occurred in 25 min between the hours 19:40 and 20:05. The total amount of rain was 52.5 mm.

The HEC-RAS 4.0 software of the Hydrology Engineering Center (USA) is used to perform the hydraulic analysis of the sub-area of interest in the catchment area of a length 117 m. This area consists of an existing stoned bridge (culvert box). The HEC-RAS 4.0 software was used to compute water surface elevations at selected locations for a given set of flow values. The computational procedure is based on solution of one-dimensional continuity, energy and Manning's equations using the standard step method. For carrying out the hydraulic analysis, water flow calculation was based on the flood hydrograph that corresponds with 30 October 2006, which is delimited as a storm of high magnitude of duration, with a return period of the order of 75 years. From the flood hydrographs, the largest flow is calculated, as the mean flow in time of 15 min at both sides of peak value in the hydrograph. Using a linear interpolation and by taking into account the hydrologic data of the region, maximum mean flows are calculated for a return period of time of 75, 50, 25, 10, 5 and 2 years with values of 69, 59, 48, 29, 17 and $10 \text{ m}^3 \text{ s}^{-1}$, respectively. It has been found that even with an analysis of 2 years return period, the culvert box (bridge) will overflow for the 30 October 2006 flood event conditions.

5 Results

The degree of urbanization and the development of a flood hazard map for the catchment area are the main outcomes of this study.

After applying the required pre-processing steps of remotely sensed images as shown in Sect. 3.2, the next step is to apply the classification algorithm. Indeed, for the unsupervised classification case, the overall accuracy (i.e. the number of pixels correctly assigned to a certain class divided by the total numbers of pixels automatically assigned to that class) and Kappa index is found to be 93.55% and 0.41, respectively for the Landsat TM images acquired in 2000, 2001 and 2008. Kappa index is very similar to the overall accuracy, but it introduces a chance agreement. Indeed, a zero value would indicate that the classification agrees with the reference as bad as an aleatory classification. Such Kappa index is in agreement with the recommended value by Lucas et al. (1994). For the high-resolution images (2003 and 2006), the overall accuracy is more than 96%. These results are in a general agreement and fulfill the requirements of the national land use inventory. The mean error for unsupervised classification is 0.358 and has been applied to the old image acquisitions such as 1985 and 1987. A direct comparison between the areas in square

Table 1. Determined urbanization factors for each image.

Data	Urbanization Factor (building activities) (%)
Air-Photos	
Air Photo – 1963	0.9
Satellite Images	
(Landsat TM-5) 3 Jun 1985	6.0
(Landsat TM-5) 29 Sep 1987	7.2
(LandsatETM+7) 30 May 2000	11.8
(LandsatETM+7) 30 Jan 2001	12.2
(LandsatETM+7) 19 Dec 2008	33.0
(Quickbird) 2003	16.0
(Quickbird) 2006	27.0

meters obtained by using the spectral signatures obtained from the recent spectro-radiometric measurements of the same type of class is made and the area assigned from the automatic classification. Indeed, a 10% difference is found. Based on these accuracy assessment tests, the next step is to obtain the degree of urbanization from the implementation of classification process. Table 1 presents the degree of urbanization (buildings, road infrastructure = urban area) based on the results found by applying the unsupervised classification technique. The urbanization ranged from 0.9 to 33% from 1963 to 2008, respectively. There is a significant change in the building activities that have been occurred in the last 7 years, especially for the Tala area. The estimated number of buildings for Kissonerga Village for the 1982 and 2002 were 256 and 355, respectively (38.5% increase) based on the statistical data provided by the local authorities. The urbanization factors found from the classified images acquired in 1985 and 2003 (the nearest dates), are 6 and 16%, respectively (i.e. 38.5% increase). It is apparent that the results obtained both from the remotely sensed images and from the statistical records are very similar.

As it has been described in the methodology, the next step in order to develop a flood hazard map is to apply a hydraulic model. Indeed, a three dimensional hydraulic representation of a sub-region of the catchment area is performed. The return period of the flood has been estimated to be 75 years using the existing meteorological data found during the 30 October 2006 flood event. The maximum flow of water has been calculated for several periods of years. The existing return period of the 2006 flood was characterized as “75 years return period event”. Therefore, the only parameter that may affect the area is coming only from the urbanization effects. By neglecting other factors used to flood analysis; the results in this stage are treated as indicative rather than definitive. A flood map of the area under investigation is produced and the urban areas that appeared to be at highest risk are considered. The author used the demographic data

that were available in 2002 for all the villages around the area under investigation. The “Hydrologic Modelling System” software was used to perform the hydraulic analysis as reported in Sect. 4. It has been found that even with hydraulic analysis of 2-years return period, the culvert box (bridge) will overflow for the 30 October 2006 prevailing structural conditions.

Flood depth is considered as the most important indicator of the intensity of flood hazard (Townsend et al., 1998). A flood hazard map is prepared based on the estimated depth of inundation for a fifty-year flood by simulating the path of over bank flow from the main channel to the adjacent flood plain. Taking risk as a function of hazard and vulnerability, a ranking matrix of three-dimensional multiplication mode (Islam and Sado, 2002) is used to obtain the risk factors taking into account the interactive effect of flood area and depth, population density and land-use/land-cover type. Indeed, it has been found that the highest flood risky area in comparison with the other areas was the Tala village.

6 Conclusions

The importance of monitoring urban growth on catchment areas using remote sensing has been highlighted. The results clearly illustrate that tremendous urban development has taken place from 1963 to 2008 for the Agriokalamini catchment area in Paphos District area (Cyprus). Inevitably, the urban lands increased the pressure of the drainage systems. A flood risk assessment was performed. Indeed, Tala Village area was found to be the most high-risky area than the others in terms of its impact in the catchment’s area. A flood risk map was developed using GIS software for a fifty-year flood considering inundation area, flood depth, land use type and population affected. Future work will consist of carrying out flood risk assessment analysis by using full hydraulic data for all the catchment areas in Cyprus. The classification accuracy can be improved when accurate ancillary information from GIS parcels and the knowledge of more class information become available. The study of the October’s flood event shows that, in addition to natural processes, human activities driven by socio-economic factors may be responsible for the recently increasing level of flood risks.

Acknowledgements. The author wishes to acknowledge the Cyprus University of Technology (<http://www.cut.ac.cy/>) for supporting this study.

Edited by: S. Michaelides, K. Savvidou, and F. Tymvios
Reviewed by: A. Retalis and two other anonymous referees

References

- Brath, A., Montanari, A., and Moretti, G.: Assessing the effect on flood frequency of land use change via hydrological simulation, *J. Hydrol.*, 324, 141–153, 2006.
- Hadjimitsis, D. G., Clayton, C. R. I., and Hope, V. S.: An assessment of the effectiveness of atmospheric correction algorithms through the remote sensing of some reservoirs, *Int. J. Remote Sens.*, 25(18), 3651–3674, 2004a.
- Hadjimitsis, D. G., Clayton, C. R. I., and Retalis, A.: Darkest pixel atmospheric correction algorithm: a revised procedure for environmental applications of satellite remotely sensed imagery, *Proceedings 10th International Symposium on Remote Sensing, Proc. SPIE 5239*, p. 464, 2004b.
- Hadjimitsis, D. G.: The use of satellite remote sensing and GIS for assisting flood risk assessment: a case study of Agriokalamini Catchment area in Paphos-Cyprus, *Proceedings of the SPIE, 6742, 67420Z.1–67420Z.7*, 2007.
- Hadjimitsis, D. G. and Themistocleous, K.: Assessment of the effectiveness of atmospheric correction methods using standard calibration targets, ground measurements and ASTER images, *Proceedings of the SPIE 7475*, p. 74750V, 2009.
- Hsiao, K. S., Lau, C. C., and Hsu, W. C.: Various classification methods for rice paddy classification, *Photogramm. Eng. Rem. S.*, 9(1), 13–26, 2004.
- Islam, M. M. and Sado, K.: Development priority map for flood countermeasures by remote sensing data with Geographic Information System, *J. Hydrol. Eng.*, 7(5), 346–355, September/October 2002.
- Khan, S. D.: Urban development and flooding in Houston Texas, inferences from remote sensing data using neural network technique, *Environ. Geol.*, 47, 1120–1127, 2005.
- Lucas, I. F. J., Frans, J. M., and Wel, V. D.: Accuracy assessment of satellite derived land-cover data: a review, *Photogramm. Eng. Remote Sens.*, 60, 410–432, 1994.
- Masek, J. G., Lindsay, F. E., and Goward, S. N.: Dynamics of urban growth in the Washington DC metropolitan area, 1973–1996, from Landsat observations, *Int. J. Remote Sens.*, 21, 3473–3486, 2000.
- Mather, P. M.: *Computer processing of remotely-sensed images. An Introduction*, Chichester: Wiley, ISBN 0-471-98550-3, 2004.
- Moeller, M.: *Remote Sensing for the Monitoring of Urban Growth Patterns*, in: *The International Archives of the Photogrammetry*, edited by: Moeller, M. and Wentz, E., *Remote Sensing and Spatial Information Sciences, XXXVI – 8/W27*, on CD, ISSN 1682-1777, 2005.
- Niehoff, D., Fritsch, U., and Bronstert, A.: Land-use impacts on storm-runoff generation: scenarios of land-use change and simulation of hydrological response in a meso-scale catchment in SW-Germany, *J. Hydrol.*, 267, 80–93, 2001.
- Ologunorisa, E. T.: An Assessment of Flood Vulnerability Zones in the Niger Delta, Nigeria, *Int. J. Environ. Stud.*, 61, 31–38, 2004.
- Townsend, P. A. and Walsh, S. J.: Modelling flood plain inundation using integrated GIS with radar and optical remote sensing, *Geomorphology*, 21(98), 295–312, 1998.
- Zhang, X., Yu, X., Wu, S., Zhang, M., and Li, J.: Response of land use/coverage change to hydrological dynamics at watershed scale in the Loess Plateau of China, *Acta Ecologica Sinica*, 27, 414–421, 2007.